

Growth dynamics and body size evolution of South American long-necked chelid turtles: A bone histology approach

MARIA EUGENIA PEREYRA, PAULA BONA, IGNACIO ALEJANDRO CERDA, JUAN MARCOS JANNELLO, MARCELO SAÚL DE LA FUENTE, and BÁRBARA DESÁNTOLO



Pereyra, M.E., Bona, P., Cerda, I.A., Jannello, J.M., De la Fuente, M.S., and Desántolo, B. 2020. Growth dynamics and body size evolution of South American long-necked chelid turtles: A bone histology approach. *Acta Palaeontologica Polonica* 65 (3): 535–545.

Among turtles, cases of “gigantism” occur mostly in pleurodiran Pelomedusoides and cryptodirans, but are infrequent among pleurodiran chelids, which are mostly small-medium sized turtles. *Yaminuechelys* spp. are extinct South American long-necked chelids (from the Late Cretaceous–early Paleocene of Patagonia, Argentina) with carapaces almost three times larger than their extant sister taxon, *Hydromedusa tectifera*. Since evolutionary changes in size can be analyzed based on growth dynamics, we studied growth strategies from an osteohistological point of view. We sampled both extinct (*Yaminuechelys maior*) and extant (*H. tectifera*) species, in order to test hypotheses related to the mechanisms involved in the macroevolution of size within this clade. For this purpose, thin sections of long bone (humerus and femur) shafts of specimens of different ontogenetic stages for these species were prepared. The osteohistological study reveals a similar growth dynamic in both taxa, with a poorly vascularized cortex dominated by parallel-fibered bone and interrupted by lines of arrested growth (LAGs). The huge body size of *Y. maior* appears to be a consequence of the prolongation of the growth phase, suggesting that it had a longer lifespan than *H. tectifera*, allowing to reach greater sizes. In this way, and assuming that there is no displacement at the beginning of development (e.g., a delay in the earliest stages of growth) in *H. tectifera*, the acquisition of a large size in *Yaminuechelys* would be explained by hypomorphosis of the former or hypermorphosis of the latter, depending on the reconstruction of the ancestral condition of this clade.

Key words: Testudines, Chelidae, growth rate, body size, paleohistology, ontogeny, Paleocene, Argentina.

Maria Eugenia Pereyra [m.eugenia.pereyra@gmail.com] and Paula Bona [paulabona26@gmail.com], División Paleontología Vertebrados, Museo de La Plata (Unidad de Investigación Anexo), Facultad de Ciencias Naturales y Museo, Paseo del Bosque s/n, CP1900, La Plata, Buenos Aires, Argentina.

Ignacio Alejandro Cerda [nachocerda6@gmail.com], CONICET; Instituto de Investigaciones en Paleobiología y Geología, Universidad Nacional de Río Negro y Museo Carlos Ameghino, Belgrano 1700, Paraje Pichi Ruca (predio Marabunta), CP8300, Cipolletti, Río Negro, Argentina.

Juan Marcos Jannello [marcosjannello@hotmail.com] and Marcelo Saúl De la Fuente [mdelafuente1910@gmail.com], Instituto de Evolución, Ecología Histórica y Ambiente (IDEVEA-CONICET, Universidad Tecnológica Nacional, FRSR) Av. Gral. J.J. Urquiza 314, CP5600, San Rafael, Mendoza, Argentina.

Bárbara Desántolo [bdesantolo@med.unlp.edu.ar], Cátedra de Citología, Histología y Embriología A, Facultad de Ciencias Médicas, Universidad Nacional de La Plata, 60 y 122 s/n, La Plata, Buenos Aires, Argentina.

Received 11 November 2019, accepted 13 May 2020, available online 22 June 2020.

Copyright © 2020 M.E. Pereyra et al. This is an open-access article distributed under the terms of the Creative Commons Attribution License (for details please see <http://creativecommons.org/licenses/by/4.0/>), which permits unrestricted use, distribution, and reproduction in any medium, provided the original author and source are credited.

Introduction

During the Late Cretaceous and early Paleocene, Chelidae turtles were one of the most abundant and diverse groups of reptiles inhabiting freshwater ecosystems in Patagonia (e.g., Bona et al. 2009; Sterli and De la Fuente 2013; De la Fuente et al. 2014). These pleurodiran turtles form a Gondwanic clade,

distributed in South America and Australasia, that survived the K-Pg boundary (Pritchard and Trebbau 1984; Bona et al. 2009; Sterli and De la Fuente 2013; De la Fuente et al. 2014; Maniel and De la Fuente 2016). Within this clade, the monophyly of the long-necked chelids is still under discussion (Gaffney 1977; Pritchard 1988; Seddon et al. 1997; Georges et al. 1998; Bona and De la Fuente 2005; Guillon et al. 2012; De

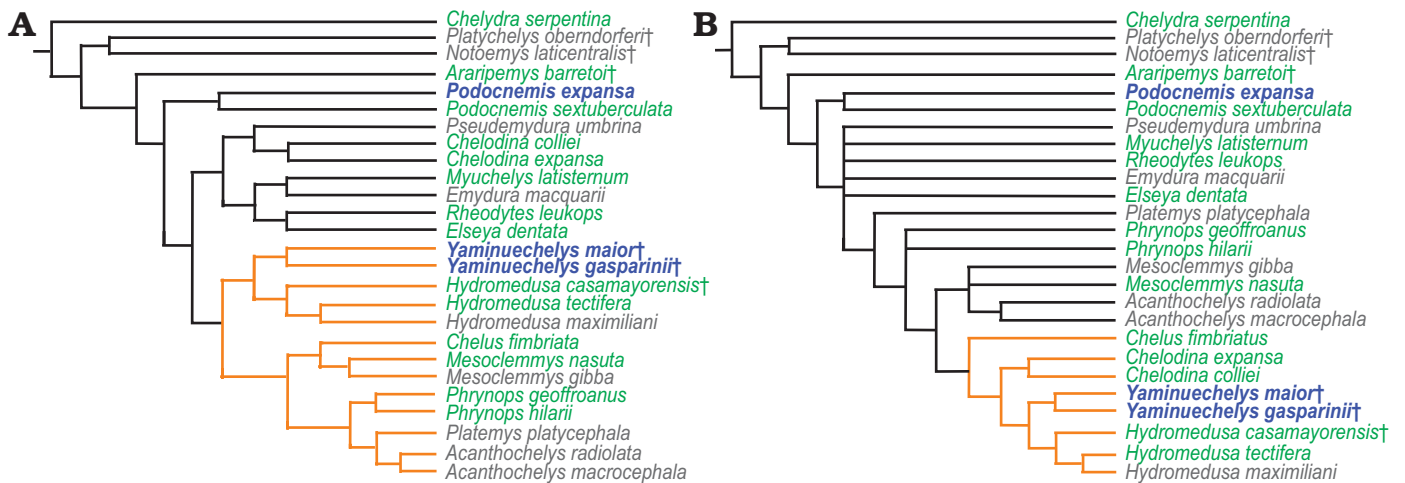


Fig. 1. Size distribution of chelid turtles represented in two different phylogenetic hypotheses from Maniel et al. (2018). Both topologies recover two alternative hypotheses (orange): the monophyly of the South American chelid clade (A) and the monophyly of the of the long necked chelid turtles (B) (see Maniel et al. 2018, for more information). Grey, species smaller than 20 cm; green, 20–60 cm; blue and bold, larger than 60 cm. The size is based on the carapace length.

la Fuente et al. 2017a; Maniel et al. 2018). Several phylogenetic proposals based on morphological data support the monophyly of the South American long-necked chelids represented by *Chelus fimbriata* (Schneider, 1783) and the crown group “*Hydromedusa* Wagler, 1830 + *Yaminuechelys* De la Fuente, De Lapparent de Broin, and Manera de Bianco, 2001” (Bona and De la Fuente 2005; De la Fuente et al. 2015, 2017a; Maniel et al. 2018) (Fig. 1). The extinct *Yaminuechelys* is recorded from the Late Cretaceous to the early Paleocene in Patagonia (Bona 2004, 2006; Bona and De la Fuente 2005; Bona et al. 2009; De la Fuente et al. 2015) with *Yaminuechelys gasparini* De la Fuente, De Lapparent de Broin, and Manera de Bianco, 2001 and *Y. maior* (Staesche, 1929). *Yaminuechelys maior* is one of the largest chelids known, with carapaces that reach almost a meter in length (Bona et al. 2009).

Cases of “gigantism” occur among turtles mostly in cryptodirans and pleurodiran Pelomedusoides (Hermanson et al. 2017), but are infrequent among chelids. With the exception of a few cases in the fossil record (e.g., the upper Campanian–lower Maastrichtian *Mendozachelys wichmanni* De la Fuente, Maniel, Jannello, Sterli, Riga, and Novas, 2017b and the lower Paleocene *Y. maior*), chelids are medium to small sized turtles. As an example, the extant *Hydromedusa tectifera* Cope, 1868 has carapaces 20 to 30 cm long and *Phrynops hilarii* (Duméril and Bibron, 1835) about 46 cm long (Benefield 1979; Pritchard 1979; Chinen et al. 2004). The adult specimens of *Y. maior* have carapaces that grade between 60 and 80 cm long (e.g., Bona and De la Fuente 2005). The fact that during the last 64 million years chelid species did not grow beyond a half meter length is an interesting issue to be addressed. In this context, the case of *Y. maior* and the mechanisms that led this species to be “giant” constitute a potentially informative way to tackle the evolution of size variation in turtles. In this regard, growth dynamics are a key factor to analyse the evolution of size variation in vertebrates (e.g., Sander et al. 2004).

Growth dynamics in fossil vertebrates can be assessed from long bone histology (Erickson 2014). Several osteohistological studies published during the last decades have focused on growth dynamics of several extinct taxa (e.g., De Ricqlès 1976; Reid 1983, 1996; Castanet and Smirina 1990; Sander et al. 2004; Cerda et al. 2017). However, fossil turtles have not been properly analysed and studies related to growth dynamics and life history have focused on living taxa (e.g., Rhodin 1985; Shine and Iverson 1995; Zug et al. 1995, 2006; Coles et al. 2001; Goshe et al. 2010; Prieto et al. 2013). Histological analyses on fossil turtles have been mostly done on shell bones (e.g., Scheyer and Sánchez-Villagra 2007; Scheyer et al. 2014a, b; Jannello et al. 2016; De la Fuente et al. 2017a, b; Maniel et al. 2018). Furthermore, with the exception of a few works (e.g., Enlow and Brown 1956; Suzuki 1963; Enlow 1969; De Ricqlès 1976; Chinsamy and Valenzuela 2008; Bailleul et al. 2011; Pereyra et al. 2019), most of the published contributions on the long bone histology of living and extinct turtles focused on the number and distribution of growth marks, leaving other histological parameters (e.g., collagenous fibre arrangement in the primary bone matrix, vascular density, and vascularization pattern) poorly studied.

Here we provide a detailed histological analysis of the long bones of the extinct *Yaminuechelys* and the extant *Hydromedusa*. Our main goals are to (i) recognize changes during ontogeny and (ii) identify the main mechanisms related to the phyletic body size increase in *Yaminuechelys*. The data presented here provide new evidence on the macroevolution of body size in long-necked chelid turtles.

Institutional abbreviations.—MLP, Museo de La Plata, La Plata, Argentina; MLPR, Herpetological collection, Museo de La Plata, La Plata, Argentina; MPEF-PV, Paleovertebrates collection, Museo Paleontológico Egidio Feruglio, Trelew, Argentina.

Other abbreviations.—LAGs, lines of arrested growth.

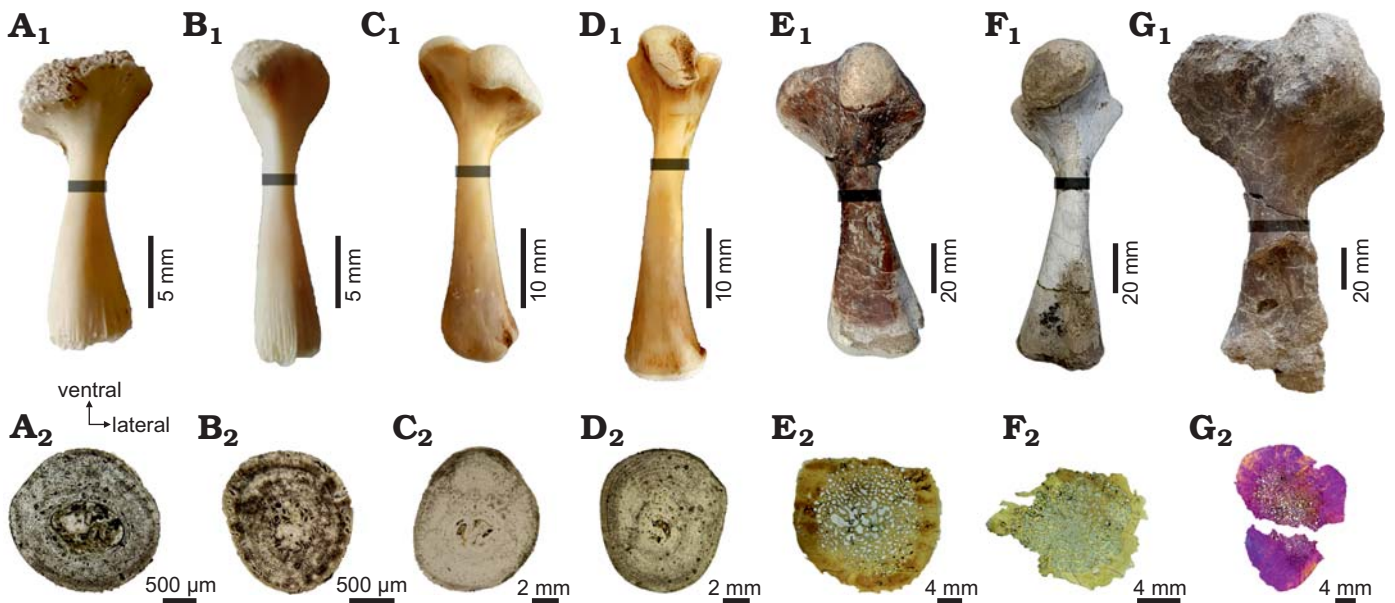


Fig. 2. Stylopodial bones of chelid turtles sampled in this study, showing the position where the thin sections were obtained (gray bar) and the complete shaft section in each element. **A–D.** *Hydromedusa tectifera* Cope, 1869; Recent, La Plata, Buenos Aires province, Argentina. **A.** MLPR-6291, dorsal view of the left humerus (A_1), cross section (A_2). **B.** MLPR-6291, dorsal view of the left femur (B_1), cross section (B_2). **C.** MLPR-6411, dorsal view of the right humerus (C_1), cross section (C_2). **D.** MLPR-6411, dorsal view of the right femur (D_1), cross section (D_2). **E–G.** *Yaminuechelys maior* (Staesche, 1929); Cerro Hansen, Danian of Salamanca Formation, Chubut Province, Argentina. **E.** MPEFPV-599, dorsal view of the right humerus (E_1), cross section (E_2). **F.** MPEFPV-599, dorsal view of the left femur (F_1), cross section (F_2). **G.** MLP-14-9-23-1, dorsal view of the left humerus (G_1), cross section (G_2). Note that the expansion of the medullary region is higher in *Y. maior* than in *H. tectifera* (see discussion in the text).

Material and methods

Two juveniles (MLPR-6291, MLPR-6747) and one adult (MLPR-6411) of Recent *Hydromedusa tectifera* were analysed (Fig. 2A₁–D₁). Specimens were found dead, the adult in fresh condition and the juveniles dried; they were a priori ontogenetically classified based on the total length of the carapace (Table 1). The stylopodia (humerus and femur) of each individual were manually defleshed, boiled with a detergent solution and air-dried. Fossil material of *Yaminuechelys maior* (MPEFPV-599 and MLP-14-9-23-1; see Table 1) here analysed come from the upper levels of the Salamanca Formation (Banco Negro Inferior), with a Danian age (early Paleocene), which outcrops along the coast of the Chubut Province, Patagonia, Argentina (see

Bona and De la Fuente 2005; Sterli and De la Fuente 2013). A humerus and femur of a subadult (MPEFPV-599) and a humerus of an adult (MLP-14-9-23-1) of *Y. maior* were studied (Fig. 2E₁–G₁). The relative ontogenetic stages of individuals of *H. tectifera* and *Y. maior* were a priori determined on the basis of their carapace length following Benefield (1979) and Pritchard (1979). Although in reptiles the size may vary between specimens of the same stage, usually an adult stage is assigned to the maximum known size. In the case of turtles, the relative size (i.e., antero-posterior length) of the carapaces is usually used a priori as an estimator of the general ontogenetic stage (juvenile, subadult, adult). In the case of fossils, there are usually few specimens available, making this estimation even more speculative. In the present case, the larger specimens of *Y. maior* reach 60–80 cm of cara-

Table 1. Specimens and skeletal bones examined for osteohistology.

Specimen ID	Age group	Locality	Condition	Carapace length (mm)	Skeletal element	Length (mm)	Visible LAGs
<i>Yaminuechelys maior</i> (MLP-14-9-23-1)	adult	Danian, Salamanca Formation; Cuenca del Golfo San Jorge	–	~600	left humerus	~180	29
<i>Yaminuechelys maior</i> (MPEFPV-599)	subadult		–	~300	right humerus	130	44
					left femur	130	6
<i>Hydromedusa tectifera</i> (MLPR-6411)	adult	Recent, La Plata	fresh	217	right humerus	43.4	22
					right femur	49.83	12
<i>Hydromedusa tectifera</i> (MLPR-6291)	juvenile	Recent, Villa Montoro, La Plata	dry	117	left humerus	18.51	2
					left femur	21.9	2
<i>Hydromedusa tectifera</i> (MLPR-6747)	juvenile	Recent, locality unknown	dry	85	left humerus	16	–
					left femur	15.5	1

pace length. Based on this information, the MPEFPV-599 (~30 cm length, Table 1) was hypothesized as a subadult and the MLP-14-9-23-1 (~60 cm length, Table 1) as an adult. These hypotheses were then tested through osteohistological analyses (see below).

For histological analyses, a single thin section from one humerus and one femur of each specimen has been sampled. Planes of sectioning were located at the minimum diaphyseal circumference (Fig. 2) to capture a cross-section at the growth centre (sensu Nakajima et al. 2014). The growth centre contains the longest record of an individual's growth. Therefore, errors resulting from growth variations are reduced. Prior to sectioning, each bone was photographed and measured using a calliper. The lengths were measured from the most proximal surface of the long bone head to the most distal condyle. The extant and extinct specimens were prepared using standard procedures for undecalcified bones (Chinsamy and Raath 1992). The bones were embedded in epoxy resin (DICAST® LY 554) with a catalyst (DICURE® HY 554) and placed on heat for one day. Blocks approximately 3 cm-thick were transversally cut using a custom diamond saw under refrigeration with soluble oil. One side of these blocks was ground and polished with 180-grit silicon carbide abrasive powder using a custom grinding machine. This side of the block was then painted with the same epoxy resin and catalyst for the infiltration of the porosity of the bone. The "mounting-side" was polished with 400-grit silicon carbide abrasive powder using the grinding machine until the surface was completely flat, smooth, and free from scratch marks. The polished slices were then washed, dried and mounted onto frosted glass slides with epoxy resin (DICAST® LY 867) and a catalyst (DICURE® HY 867) for the fossil materials, and, for the extant specimens, an ultraviolet curing glue (Trabasil® NR2). Approximately 2 mm-thick blocks were cut and then grounded and polished with silicon carbide powder of decreasing coarseness (220–800-grit) using a custom grinding machine. In addition to machine grinding, some manual grinding was done to make the surface thinner. The thin section slides were not cover-slipped. The thin sections were examined under polarized and ordinary light with 4×, 10×, and 20× objectives using an Optiphot-Pol 255884 (Nikon Instruments Inc.) polarizing microscope with cross-polarizer (530 nm) and a 1/4 lambda plate. Images were obtained with a digital camera (smartphone Samsung S6 edge). The terminology and definitions of histological structures used in this study are from Francillon-Vieillot et al. (1990).

The preparation of the histological sections was carried out in the Museo Provincial Carlos Ameghino (Rio Negro, Argentina), in the Museo de Historia Natural de San Rafael (Mendoza, Argentina), in the Centro de Investigaciones Geológicas (CIG), and in the Ponti's geological laboratory. The analysis of all the slices was performed in the Museo de La Plata and in the Instituto de Recursos Minerales (INREMI).

The analyses and measurements taken from the photo-

graphs of the slices were processed with the software ImageJ (Rasband 2003). In *Hydromedusa tectifera*, the annual and daily bone appositional rates and the rate of growth were measured following the procedure proposed by Woodward et al. (2014). Two daily bone appositional rates were obtained: one dividing the annual bone appositional rate by an estimated 240 active growing days in a year and the other considering 365 active growing days in a year (Lescano et al. 2008; Bonino et al. 2009). As the circumference of the first line of arrested growth (LAG) in all specimens here analysed is equal to the circumference of the midshaft at the time of hatching (an expansion of the medullary region was not observed in the last stage sampled here; see SOM: table 1, Supplementary Online Material available at http://app.pan.pl/SOM/app65-Pereyra_etal_SOM.pdf), the age of each specimen was estimated by the count of the observed LAGs. In the case of *Y. maior*, the annual appositional rate and the growth rate were estimated using the same method but measured only in the dorsal area of the humerus, which, due to diagenetic alterations of the other parts, is the only region where the cortices preserve LAGs. The estimations of the day count per year for the Paleocene is ~371 (Wells 1963); therefore, for the daily bone appositional rates in *Y. maior*, we made calculations for both 249 and 371 growing days in a year. The value of 249 days of growth came up from a calculation based on the 240 growing days reported by Lescano et al. (2008) and Bonino et al. (2009) for *H. tectifera*.

Results

Stylopodial bone microstructure of *Yaminuechelys*

maior.—*Humerus*: The medullary region is wide and occupied by trabecular bone (the percentage of the cross section occupied by the medullary cavity in this species was 69% for the subadult and 80% for the adult). Whereas in the adult (MLP-14-9-23-1) the cortex becomes narrower towards the dorsal area, the cortical thickness appears to be relatively homogeneous in the subadult (MPEFPV-599) (though this cannot be assessed with certainty since the ventral area was not preserved). Abundant resorption spaces are observed from the perimedullary margin to the middle cortex (Fig. 3A₁, B₁). These spaces decrease in size towards the outer cortex. The primary bone is mostly formed by parallel-fibered/lamellar bone tissue (Fig. 3A₂, B₂). Crossed parallel-fibered bone tissue (i.e., the intrinsic fibres exhibit two main orientations; parallel and concentric to the shaft main axis) is observed in MPEFPV-599 (Fig. 3A₃). The degree of organization of the intrinsic fibres tends to increase towards the outer cortex (Fig. 3A₂, B₂), being particularly well organized in the dorsal area. The cortex is vascularized with mostly longitudinal canals. The density of the simple vascular canals is relatively higher in MPEFPV-599 compared to MLP-14-9-23-1. Whereas the vascular density and distribution are rather homogeneous in the MPEFPV-599 cortex, this vasculature is restricted to the perimedullary re-

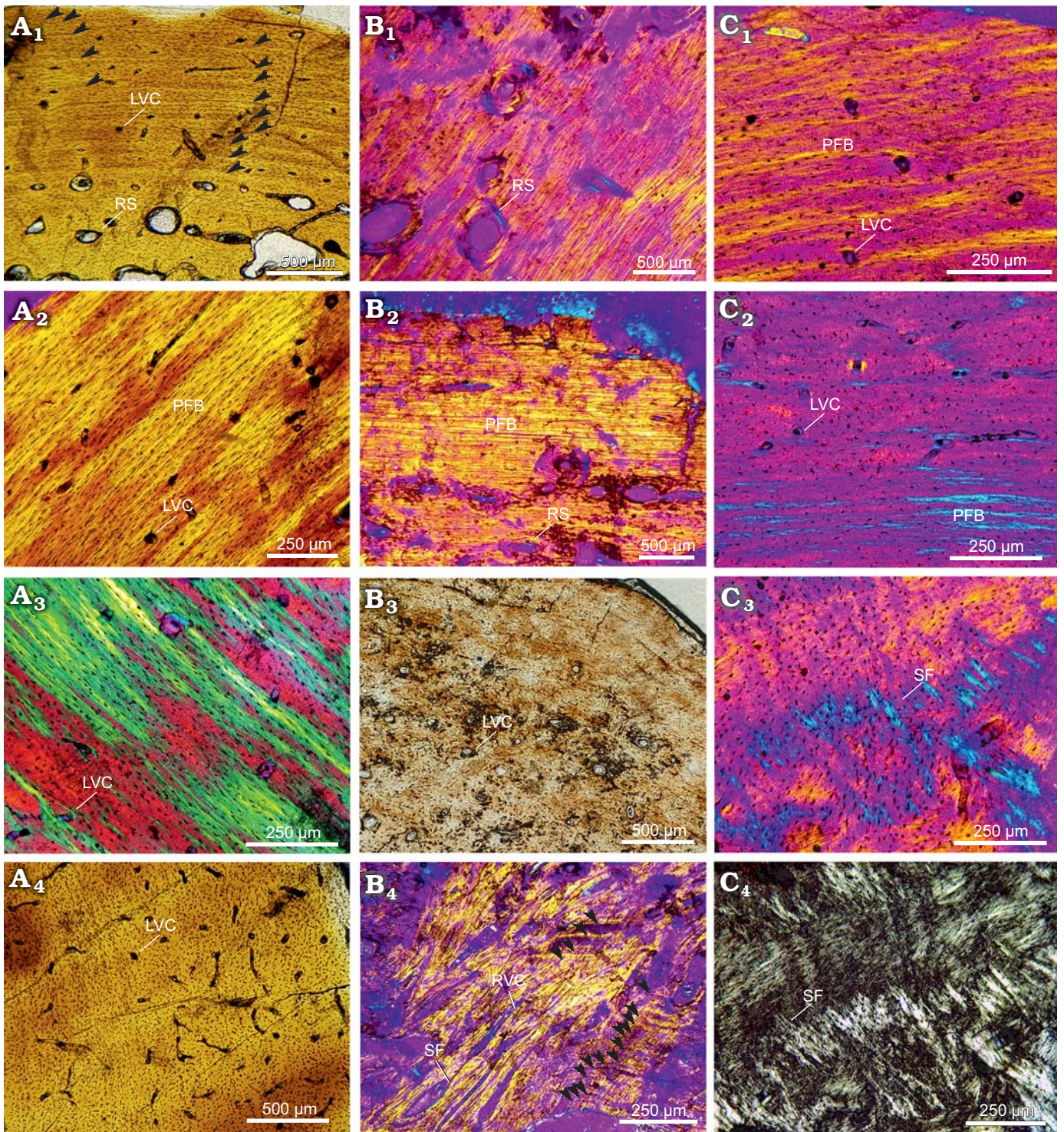


Fig. 3. Stylopodial bone histology of chelid turtle *Yaminuechelys maior* (Staesche, 1929), Cerro Hansen, Danian, Paleocene of Salamanca Formation, Chubut Province, Argentina (Bona and De la Fuente 2005). **A.** MPEFPV-599, humerus: dorsal (A₁), dorsomedial (A₂), dorsolateral (A₃), and lateral (A₄) areas. **B.** MLP-14-9-23-1, humerus: lateral (B₁), dorsal (B₂), medial (B₃), and ventral (B₄) areas. Arrowheads in A₁ and B₄ indicate lines of arrested growth. **C.** MPEFPV-599, femur: dorsal (C₁), dorsolateral (C₂), and ventral (C₃, C₄) areas. Photographs under normal light (A₁, A₄, B₃), under polarized light (C₄), under polarized light with lambda compensator (A₂, A₃, B₁, B₂, B₄, C₁–C₃). Abbreviations: LVC, simple longitudinal vascular canals; PFB, parallel-fibered bone; RS, resorption cavities; RVC, simple radial vascular canals; SF, Sharpey's fibres.

gion in MLP-14-9-23-1 (Fig. 3A₄, B₃). The density of vascular spaces appears to be higher in the ventromedial and ventrolateral areas of the MPEFPV-599 cortex. Simple radial vascular canals that are extended from the perimedullary

region to the subperiosteal cortex are recorded in the ventral area of MLP-14-9-23-1. These radial canals are associated with a high amount of Sharpey's fibres (Fig. 3B₄). The shape and arrangement of the osteocyte lacunae is strongly vari-

able in MPEFPV-599; they are flattened and regularly distributed throughout the entire compacta in the medial and dorsomedial areas, and flattened to rounded and irregularly distributed in the other portions of the cortex (Fig. 3A₂–A₄). Conversely, osteocyte lacunae are mainly flattened and regularly distributed throughout the entire compacta of MLP-14-9-23-1 (Fig. 3B₁, B₂). Abundant Sharpey's fibres that penetrate the subperiosteal margin at an acute angle (medial and ventrolateral areas) and at a straight angle (dorsal area) are observed. Most of these fibres reach the perimedullary region. Lines of arrested growth (LAGs) are clearly observed in the whole cortex in MPEFPV-599, but only in the outer cortex in MLP-14-9-23-1 (Fig. 3A₁, B₄). These LAGs are best preserved mostly in the dorsal area in MPEFPV-599 and in the ventral area in MLP-14-9-23-1, although a distinct stratification pattern is observed; in the dorsal area of MLP-14-9-23-1, LAGs are only poorly distinguished (Fig. 3B₂). Even though diagenetic alteration precludes a confident estimation of the complete set of LAGs, at least 44 and 29 of these growth marks are evidenced in the compacta of MPEFPV-599 and MLP-14-9-23-1, respectively (SOM: fig. 3). A decrease in the spaces between successive LAGs is conspicuous towards the outer cortex in both samples.

Femur: The cortex of the subadult MPEFPV-599 surrounds a wide medullary region filled with cancellous bone. Resorption cavities are scattered. The primary bone tissue is mostly composed of crossed parallel-fibered bone. The cortex is vascularized with longitudinal canals, which exhibit a rather homogenous distribution (Fig. 3C₁). The osteocyte lacunae are predominantly rounded rather than flattened in shape (Fig. 3C₂). The lacunae are irregularly distributed throughout the entire compacta in comparison with those observed in the humerus. Sharpey's fibres are mainly observed in the dorsal area, where they penetrate in more than one main orientation (mostly at acute angles with respect to the subperiosteal margin) (Fig. 3C₃, C₄). These fibres reach the perimedullary region. A total of six LAGs could be counted (SOM: fig. 3). However, this growth mark count may be incomplete since in this cross section an important expansion of the medullary region and a significant loss of subperiosteal bone tissue are observed.

Stylopidial bone microstructure of *Hydromedusa tectifera*.—**Humerus:** The medullary region in the juveniles MLPR-6747 and MLPR-6291 is proportionally larger than in the adult MLPR-6411 (occupying 55% of the cross section in MLPR-6747, 43% in MLPR-6291, and 40% in MLPR-6411). The cortex of both specimens is narrower in the dorsal area, and the medullary region is composed of cancellous bone with a few bony trabeculae. Parallel-fibered bone tissue is the main component of the cortex. The intrinsic fibres are mostly oriented parallel to the main axis of the shaft (Fig. 4A₁, C₁, E₁). Resorption cavities are scattered in the perimedullary region, being less abundant in MLPR-6411 (Fig. 4A₂, C₂, E₂). Vascularization is more pronounced in MLPR-6291 than in the other specimens (Fig. 4A₂, C₂,

E₂). Regarding the shape of the osteocyte lacunae, these are rounded and/or flattened in different areas for each specimen (e.g., they are rounded in the whole cortical region of MLPR-6291 and in the dorsal and ventral areas of MLPR-6291 and MLPR-6411). At least 16 LAGs were counted in MLPR-6411, two in MLPR-6291 (SOM: figs. 3, 4), and none in MLPR-6747. The distance between LAGs tends to decrease towards the outer cortex, particularly in the dorsal area. Sharpey's fibres are recognized in both dorsal and ventral areas, being nevertheless more abundant in the ventral area of MLPR-6291 and MLPR-6411. These extrinsic fibres penetrate mostly at a straight angle and they almost reach the perimedullary region.

Femur: The medullary region is proportionately wider in the juvenile MLPR-6747 (46% of the cross section), intermediate in the juvenile MLPR-6291 (23%), and narrower in the adult MLPR-6411 (15%). A relative reduction of the cortex thickness in the ventral region is evident. Primary bone mainly consists of parallel-fibered bone tissue in the three specimens (Fig. 4B₁, D₁, F₁). Resorption spaces are larger and more abundant in MLPR-6747 than in the other specimens (Fig. 4B₁). These spaces are located in the perimedullary region, although in MLPR-6291 they also reach the outer cortex (Fig. 4D₁). Regarding vascularization, a higher density is observed in the ventral area. These simple vascular canals are mainly longitudinally oriented, although in MLPR-6291 some of them are radial. The canals are observed in both the middle and outer cortex. The osteocyte lacunae in MLPR-6747 are rounded in shape throughout the cortex without a particular arrangement (Fig. 4B₁). These parameters are nevertheless highly variable in specimens MLPR 6291 and MLPR-6411. A particular pattern regarding osteocyte lacunae distribution is observed in MLPR-6291 (Fig. 4B₂, D₂, F₂). In this sample, three distinct layers of cortical bone characterized by a high density of lacunae alternate with three layers where this density is strongly reduced. These layers could be interpreted as three annuli and three zones. A maximum of two LAGs, at the end of two annuli, was observed in MLPR-6291, almost 10 in MLPR-6411 (Fig. 4F₂), and one in MLPR-6747 (SOM: figs. 3, 4). Abundant Sharpey's fibres are observed through the whole cortex of MLPR-6747 (Fig. 4B₂), in the dorsal and ventral areas of MLPR-6291, and in the dorsal area of MLPR-6411.

Growth rates of *Hydromedusa tectifera* and *Yaminuechelys maior*.—Despite the fact that the activity of *Hydromedusa tectifera* does not exhibit annual interruptions, a distinct decrease in activity has been reported during autumn and winter (eight months; Lescano et al. 2008; Bonino et al. 2009). The growth rate ranges obtained for the adult *H. tectifera* (MLPR 6411) vary 0.022–0.095 mm/year in the humerus and 0.070–0.203 mm/year in the femur. Regarding the estimated daily growth rates, they range 0.06–0.26 µm/day and 0.19–0.55 µm/day in the humerus and femur, respectively, assuming an uninterrupted growth all year round. On the other hand, growth rate ranges vary 0.09–0.38 µm/day

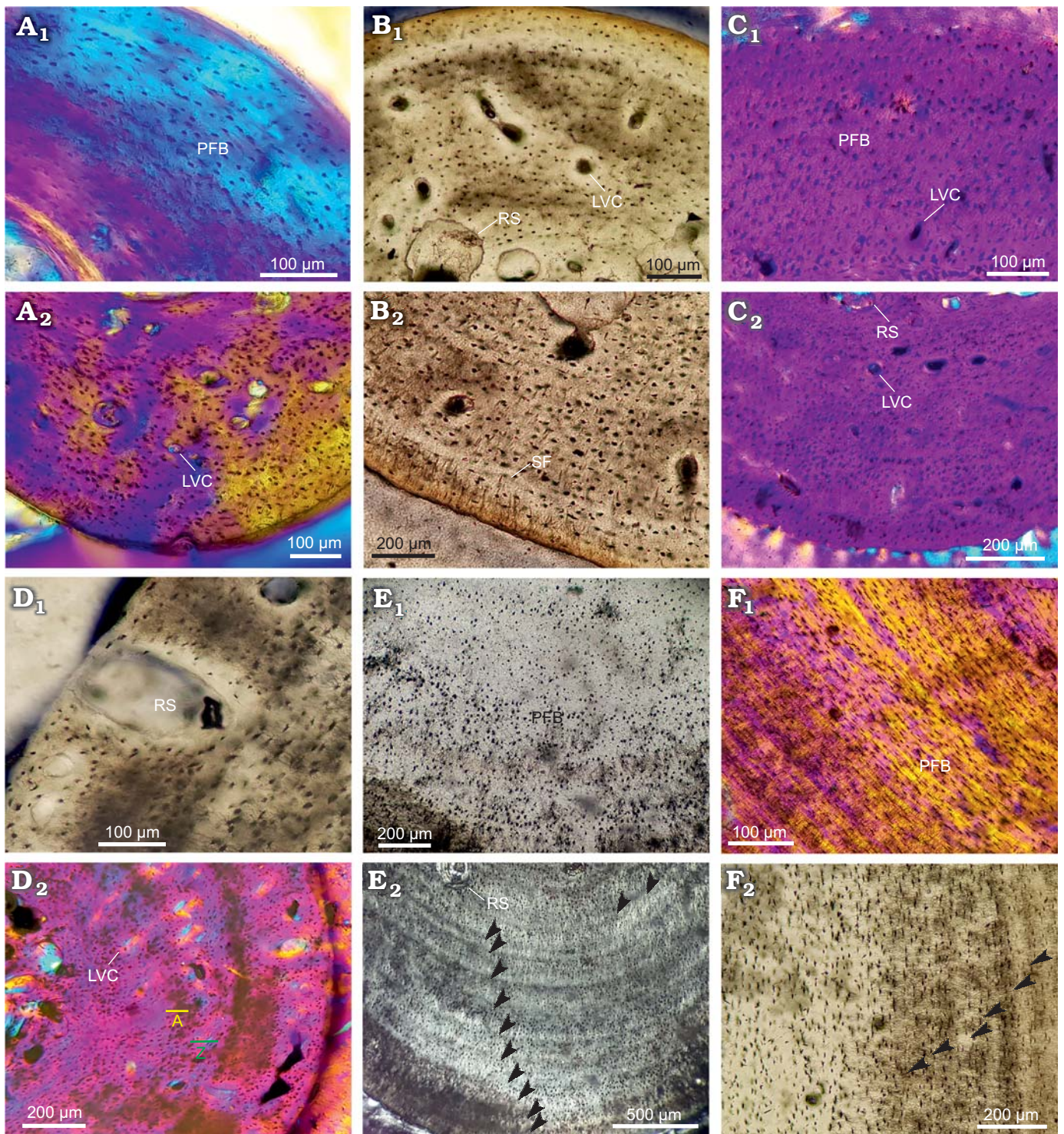


Fig. 4. Stylopodial bone histology of chelid turtle *Hydromedusa tectifera* Cope, 1869; Recent, La Plata, Buenos Aires province, Argentina. **A.** MLPR-6474, humerus: dorsolateral (A_1) and ventral (A_2) areas. **B.** MLPR-6474, femur: ventral (B_1) and dorsal (B_2) areas. **C.** MLPR-6291, humerus: dorsal (C_1) and ventral (C_2) areas. **D.** MLPR-6291, femur: lateral (D_1) and ventrolateral (D_2) areas; annuli, yellow A; zones, green Z. **E.** MLPR-6411, humerus: dorsal (E_1) and ventral (E_2) areas. **F.** MLPR-6411, femur: lateral areas (F_1 , F_2). Arrowheads in E_2 and F_2 indicate lines of arrested growth. Photographs under normal light (B_1 , B_2 , D_1 , E_1 , F_2), under polarized light (E_2), under polarized light with lambda compensator (A_1 , A_2 , C_1 , C_2 , D_2 , F_1). Abbreviations: LVC, simple longitudinal vascular canals; PFB, parallel-fibered bone; RS, resorption cavities; SF, Sharpey's fibers.

and 0.07–0.20 $\mu\text{m}/\text{day}$ in the humerus and femur, respectively, assuming a peak of growth during summer and spring (see Bonino et al. 2009; Lescano et al. 2008). The graphs of both annual and daily growth rates show an increase of these

parameters during the early stages of development and then a gradual decrease. A striking decrease in the growth rate is recorded between the eighth and twelfth year in *H. tectifera* (SOM: table 2, fig. 1). Regarding *Y. maior* (MPEFPV-599)

the inferred growth rates in the humerus vary 0.011–0.371 mm/year. Based on the work of Wells (1963), we know that one year in the Paleocene had approximately 371 days; thus, the calculated daily growth rate ranged 0.02–1 $\mu\text{m}/\text{day}$ if the turtle grew all year round, and 1.48–0.04 $\mu\text{m}/\text{day}$ if its activity peaked during summer and spring.

Discussion

After the osteohistological analysis, the ontogenetic sequences previously established (based on carapace length) for both species (*Hydromedusa tectifera* and *Yaminuechelys maior*) were corroborated by the gradual changes observed in the bone tissue patterns for the different ontogenetic stages (e.g., the pattern of distribution of the osteocyte lacunae and the degree of vascularization). Thus, in the case of fossil specimens, and based on the histology and carapace length, we observed that MPEFPV-599 is definitively younger than MLP-14-9-23-1 (Table 1). Based on the microanatomy of both species, the process of expansion of the medullary cavity in *Y. maior* is more noticeable than in *H. tectifera*, and the expansion of the medullary cavity reflects a more extended remodelling process in the extinct taxon. The percentage of the cross section occupied by the medullary cavity in the subadult of *Y. maior* is 69% while that in the adult is 80%. In consequence, the presence of a higher number of growth marks in the subadult specimen can be due to the loss of primary cortical bone (and of the LAGs deposited there) related to the expansion of the medullary cavity (higher secondary remodelling) during growth.

The different ontogenetic stages of both species here analysed exhibit a similar osteohistological pattern. Their histology revealed the presence of parallel-fibered bone with two patterns of organization of the collagen fibres: fibres in one direction (concentric or longitudinal with respect to the main axis of the bone) and fibres in two directions (concentric and longitudinal with respect to the main axis of the bone, i.e., crossed parallel-fibered bone). The osteocyte lacunae are randomly distributed mostly in earlier stages (Figs. 3 and 4). Also, the degree of vascularization is low-to-intermediate and is represented mainly by longitudinal canals. As *H. tectifera* and *Y. maior* become older, an increase of the organization of the collagen fibres and a regular distribution of the osteocyte lacunae are observed while the vascular density decreases. These variations through ontogeny in the patterns of bone histology are the expression of changes in the growth rate commonly occurring in vertebrates, which decreases while they become adults (Nagy 2000; Erickson et al. 2003; Brown et al. 2005; Klein and Sander 2007). The growth dynamics of both species fit in this model (similar growth dynamics were reported in samples of the Emydidae *Trachemys scripta elegans* Schoepff, 1792 and the Podocnemididae *Podocnemis expansa* Schweigger, 1812; Suzuki 1963; Chinsamy and Valenzuela 2008). Particularly, as *Y. maior* becomes older,

the rate of bone deposition decreases, which is reflected in the tightly grouped LAGs (Fig. 3B₂). This latter pattern is not observed in the oldest specimens of *H. tectifera*. Such osteohistological differences between species are here interpreted as evidence for a prolonged growth in *Y. maior* in comparison with the living species, a hypothesis that should be further tested with a larger sample. The same growth strategies were reported for the giant fossil crocodile *Deinosuchus* (Erickson and Brochu 1999) and the giant varanid *Megalania* (Erickson et al. 2003). In the same way, histological studies conducted on carapace bones of *Yaminuechelys* and *Hydromedusa* reveal that, whereas the former commonly exhibits numerous LAGs in the outermost area of the cortical bone, such growth marks are absent in the latter (Jannello et al. 2016; Maniel et al. 2018). This histological variation supports an extension of the growth phase in *Yaminuechelys*.

It is known that growth dynamics in vertebrates can also be interpreted by analysing growth rates throughout ontogeny (e.g., Curtin et al. 2008; Hugi and Sánchez-Villagra 2012). In our case, both species show roughly equal growth rates (SOM: fig. 1, tables 1 and 2). When analysing the mechanisms involved in the body size increase in an ancestral-descendant sequence, these osteohistological data are useful for interpretations related to heterochronic processes (e.g., Sander et al. 2004). Living chelids are small to medium sized turtles, but considering the evolutionary history of South American long-necked chelids, large sizes are the first condition registered in the fossil record, as early as the Late Cretaceous (i.e., *Yaminuechelys gasparinii*). However, in the last years new fossil material of *Hydromedusa* from the Danian of Patagonia (e.g., Maniel et al. 2018; Juliana Sterli, personal communication 2019) reveals that small-medium and large sizes co-existed in chelids from at least approximately 65 Ma. Considering this situation and the distribution of body sizes in the available phylogenetic topologies for chelid turtles (Fig. 1), the three size categories could represent the ancestral condition of the clade *Hydromedusa* + *Yaminuechelys*. Assuming all the possible ancestral conditions, and considering that there is no displacement of the onset in the development of *H. tectifera* or *Y. maior*, the evolution of body size in these turtles could be explained either by negative (hypomorphosis) or positive (hypermorphosis) shifts (sensu Reilly et al. 1997). Hypomorphosis and hypermorphosis correspond to heterochronic processes that occur between an ancestor and a descendant with the same growth rate and results in a pedomorphic (the traits of the descendant species are truncated in relation to the ancestral species) or peramorphic (the traits in the descendant species are extended relative to the ancestral species) descendant species, respectively (e.g., Reilly et al. 1997). These two hypotheses should be tested in the future, after a comprehensive analysis of the evolution of body size in pleurodiran Chelidae (as was published for cryptodirans by Vlachos and Rabi 2018).

Alongside the reported variation in the carapace and plastron size, there are also discrete morphological features

that vary during ontogeny and that could reinforce one or another hypothesis. For instance, the presence of fontanelles related to the post-hatching ossification of the carapace is a juvenile-subadult feature lost at the end of ontogeny in *Y. maior*, but persistent in adults of *H. tectifera* (SOM: fig. 2). However, adults of other *Hydromedusa* species, like *H. maximiliani* Mikan, 1820, show small sizes and a completely ossified carapace and plastron, indicating that size is independent from other morphological features that can vary during the ontogeny (Gould 1977).

Finally, the maximum yearly growth rate of *H. tectifera* (0.095 mm/year) appears to be lower than the one of *Y. maior* (0.371 mm/year). However, the minimum yearly growth rate of both species is rather similar (0.022 mm/year in *H. tectifera* and 0.011 mm/year in *Y. maior*) (SOM: table 2). The increment in the growth rate found in *Y. maior* could be interpreted in two ways. First, it could be correlated to the elevated annual temperatures estimated for the lower Paleocene (22–23°C; based on the global oceanic temperatures estimated by Zachos et al. 2008 and Hansen et al. 2013), while the annual temperatures registered today range 16–18°C (Tutiempo Network 2019). This kind of correlation was also demonstrated in other vertebrates including other turtles (Mattox 1935; Chinsamy and Venezuela 2008), amphibians (Guarino et al. 1998), and caimans (Castanet et al. 1993; Andrade et al. 2018). The growth dynamics found in this study for *Y. maior* are concordant with those reported by Case (1978) in different taxa such as mammals, birds, reptiles, and fishes, stating that there is a correlation between size and growth, where larger animals tend to present higher growth rates (Case 1978).

Finally, it is interesting to note that the male specimen of *H. tectifera* (MLPR-6411) shows a change in growth dynamics between the eighth and twelfth years of life, as evidenced by a decrease and subsequent increase of the growth rate. In other reptiles (e.g., crocodiles, Rootes et al. 1991) a decrease in the growth rate could be related to sexual maturity. Since males of chelid turtles reach sexual maturity between 11–16 years old (in *H. maximilliani*) or 4–11 years old (in Australasian chelids) (e.g., Martins and Souza 2008) the variation in growth rate observed here in MLPR-6411 could be interpreted as linked to sexual maturity. However, the subsequent increase in growth rate in this specimen may indicate that sexual maturation is not the cause of this growth pattern.

Conclusions

Here we report the first analysis of growth dynamics in chelid turtles, based on a comprehensive long bone histological analysis combining data on fossil and living species. The two taxa (*Yaminuechelys maior* and *Hydromedusa tectifera*) here analysed show similar patterns in bone microstructure. Both species have a slow growth rate reflected by the poorly vascularized parallel fibered bone matrix (with two main types of orientation for the collagen fibres), which becomes

lamellar and avascular late during ontogeny. Despite the fact that we did not sample the same ontogenetic stages in both species (i.e., *H. tectifera* specimens had not attained their maximum size), the size of our largest specimens is close to the maximum size that is known for each species. It is notable that, in the most advanced ontogenetic stage of *Y. maior*, the organization of the matrix and number of LAGs tend to be higher than in the more advanced ontogenetic stages of *H. tectifera* studied here (SOM: figs. 3, 4). The osteohistology of the available sample of *Y. maior* indicates that the large body size reached in this species could be the result of an extension of the growth phase.

Acknowledgements

We thank Marcelo Reguero, Leandro Alcalde (both MLP), and Juliana Sterli (Museo Paleontológico Egidio Feruglio, Chubut, Argentina) for collection access and permission to sample the specimens; Gabriela Guarda (La Plata, Argentina) for reviewing the English of the manuscript. Thanks, are also extended to INREMI (Instituto de Recursos Minerales, La Plata, Argentina) for the access to the polarizing microscope Nikon Optiphot-Pol 255884. We also thank Alexandra Elbakyan (Albert-Ludwigs-Universität, Freiburg, Germany), Jorge Bar (Salta, Argentina), and the Wikipaleo Group for providing literature. We are also indebted to Tomasz Szczygielski (Institute of Paleobiology, Polish Academy of Sciences, Warsaw, Poland), Nicole Klein (Steinmann Institute, University of Bonn, Germany), and the editor Olivier Lambert (Institut royal des Sciences naturelles de Belgique, Brussels, Belgium) for their very useful suggestions and comments on the original manuscript. This research was supported by Ministerio de Educación de la Nación, Incentivos-UNLP (M189 to BD), Préstamo BID ANPCyT (PICT 2015-1021 to IAC, PICT 2016-0159 to PB), and CONICET (PIP 112201301-00733 to PB).

References

- Andrade, R.C.L.P.D., Sena, M.V.A., Araújo, E.V., Bantim, R.A.M., Riff, D., and Sayão, J.M. 2018. Osteohistological study on both fossil and living Caimaninae (Crocodyliformes, Crocodylia) from South America and preliminary comments on growth physiology and ecology. *Historical Biology* 32: 346–355.
- Bailleul, A., Ségalen, L., Buscalioni, A.D., Cambra-Moo, O., and Cubo, J. 2011. Palaeohistology and preservation of tetrapods from Las Hoyas (lower cretaceous, Spain). *Comptes Rendus Palevol* 10: 367–380.
- Benefield, J. 1979. Hatching the Argentine snake-necked turtle. *International Zoo Yearbook* 19: 55–58.
- Bona, P. 2004. *Sistemática y biogeografía de las tortugas y los cocodrilos paleocenos de la Formación Salamanca, provincia de Chubut, Argentina*. 200 pp. Tesis Doctoral, Facultad de Ciencias Naturales y Museo de La Plata, Universidad Nacional de La Plata, La Plata.
- Bona, P. 2006. Paleocene (Danian) chelid turtles from Patagonia, Argentina: taxonomic and biogeographic implications. *Neues Jahrbuch für Geologie und Paläontologie Abhandlungen* 241: 303–323.
- Bona, P. and De La Fuente, M.S. 2005. Phylogenetic and paleobiogeographic implications of *Yaminuechelys maior* (Staesche, 1929) new comb., a large long-necked chelid turtle from the early Paleocene of Patagonia, Argentina. *Journal of Vertebrate Paleontology* 25: 569–582.
- Bona, P., Heredia, S., and De La Fuente, M.S. 2009. Tortugas continentales (Pleurodira: Chelidae) en la Formación Roca (Daniano), provincia de Río Negro, Argentina. *Ameghiniana* 46: 255–262.

- Bonino, M., Lescano, J., Haro, J., and Leynaud, G. 2009. Diet of *Hydromedusa tectifera* (Testudines-Chelidae) in a mountain stream of Córdoba province, Argentina. *Amphibia-Reptilia* 30: 545–554.
- Brown, T.K., Nagy, K.A., and Morafka, D.J. 2005. Costs of growth in tortoises. *Journal of Herpetology* 39: 19–23.
- Case, T.J. 1978. Speculations on the growth rate and reproduction of some dinosaurs. *Paleobiology* 4: 320–328.
- Castanet, J. and Smirina, E.M. 1990. Introduction to the skeletochronological method in amphibians and reptiles. *Annals of Sciences Natural Zoology* 11: 191–196.
- Castanet, J., Francillon-Vieillot, H., Meunier, F.J., and De Ricqlès, A. 1993. Bone and individual aging. In: B.K. Hall (ed.), *Bone* 7, 245–283. CRC Press, Boca Raton.
- Cerda, I.A., Chinsamy, A., Pol, D., Apaldetti, C., Otero, A., Powell, J.E., and Martínez, R.N. 2017. Novel insight into the origin of the growth dynamics of sauropod dinosaurs. *Plos One* 12: e0179707.
- Chinen, S., Lisboa, C.S., and Molina, F.B. 2004. Biología reproductiva de *Hydromedusa tectifera* em cativo (Testudines, Chelidae). *Arquivos do Instituto Biológico* 71: 401–403.
- Chinsamy, A. and Raath, M.A. 1992. Preparation of fossil bone for histological examination. *Palaeontology Africans* 29: 39–44.
- Chinsamy, A. and Valenzuela, N. 2008. Skeletochronology of the endangered side-neck turtle, *Podocnemis expansa*. *South African Journal Science* 104: 311–314.
- Coles, W.C., Musick, J.A., and Williamson, L.A. 2001. Skeletochronology validation from an adult loggerhead (*Caretta caretta*). *Copeia* 2001: 240–242.
- Cope, E.D. 1868. On the origin of genera. *Proceedings of the Academy of Natural Sciences of Philadelphia* 18: 242–300.
- Cope, E.D. 1869. Seven contribution to the herpetology of tropical America. *Proceedings of the American Philosophical Society* 11: 147–169.
- Curtin, A.J., Zug, G.R., Medica, P.A., and Spotila, J.R. 2008. Assessing age in the desert tortoise *Gopherus agassizii*: testing skeletochronology with individuals of known age. *Endangered Species Research* 5: 21–27.
- De la Fuente, M.S., De Lapparent de Broin, F., and Manera de Bianco, T. 2001. The oldest and first nearly complete skeleton of a chelid, of the *Hydromedusa* group (Chelidae, Pleurodira), from the Upper Cretaceous of Patagonia. *Bulletin de la Société géologique de France* 172: 237–244.
- De la Fuente, M.S., Maniel, I.J., Jannello, J.M., Filippi, L.S., and Cerda, I. 2015. Long-necked chelid turtles from the Campanian of northwestern Patagonia with comments on K/P survivorship of the genus *Yaminuechelys*. *Comptes Rendus Palevol* 14: 563–576.
- De la Fuente, M.S., Maniel, I.J., Jannello, J.M., Sterli, J., Garrido, A.C., García, R.A., Salgado, L., Canudo, J.I., and Bolatti, R. 2017a. Unusual shell anatomy and osteohistology in a new Late Cretaceous panchelid turtle from northwestern Patagonia, Argentina. *Acta Palaeontologica Polonica* 62: 585–601.
- De la Fuente, M.S., Maniel, I., Jannello, J.M., Sterli, J., Riga, B.G., and Novas, F. 2017b. A new large panchelid turtle (Pleurodira) from the Loncoche Formation (upper Campanian–lower Maastrichtian) of the Mendoza Province (Argentina): Morphological, osteohistological studies, and a preliminary phylogenetic analysis. *Cretaceous Research* 69: 147–168.
- De la Fuente, M.S., Sterli, J., and Maniel, I. 2014. *Origin, Evolution and Biogeographic History of South American Turtles*. 168 pp. Springer Earth System Sciences, Dordrecht.
- De Ricqlès, A. 1976. On bone histology of fossil and living reptiles, with comments on its functional and evolutionary significance. In: A. d'A. Bellairs and C.B. Cox (eds.), *Morphology and Biology of Reptiles*, 123–150. Academic Press, London.
- Duméril, A.M.C. and Bibron, G. 1835. *Erpétologie Générale ou Histoire Naturelle Complète des Reptiles*. Tome Second. *Librairie Encyclopédique de Roret*, Paris 2: 13–24.
- Enlow, D.H. 1969. The bone of reptiles. In: E.C. Gans (eds.), *Biology of the Reptilia*, 45–80. Academic Press, New York.
- Enlow, D.H. and Brown, S.O. 1956. A comparative histological study of fossil and recent bone tissues. Part III. *The Texas Journal of Science* 10: 187–230.
- Erickson, G.M. 2014. On dinosaur growth. *Earth and Planetary Sciences* 42: 675–697.
- Erickson, G.M. and Brochu, C.A. 1999. How the “terror crocodile” grew so big. *Nature* 398: 205–206.
- Erickson, G.M., De Ricqlès, A., De Buffrénil, V., Molnar, R.E., and Bayless, M.K. 2003. Vermiform bones and the evolution of gigantism in *Megalania*—how a reptilian fox became a lion. *Journal of Vertebrate Paleontology* 23: 966–970.
- Francillon-Vieillot, H., De Buffrénil, V., Castanet, J., Géraudie, J., Meunier, F.J., Sire, J.Y., Zylberberg, L., and De Ricqlès, A. 1990. Microstructure and mineralization of vertebrate skeletal tissues. In: J.G. Carter (eds.), *Skeletal Biomineralization: Patterns, Processes and Evolutionary Trends*, Vol. 1, 471–530. Van Nostrand Reinhold, New York.
- Gaffney, E.S. 1977. The side-necked turtle family Chelidae: a theory of relationships using shared derived characters. *American Museum Novitates* 2620: 1–28.
- Georges, A., Birrell, J., Saint, K.M., McCord, W., and Donnellan, S.C. 1998. A phylogeny for side-necked turtle (Chelonina: Pleurodira) based on mitochondrial and nuclear gene sequence variation. *Biological Journal of the Linnean Society* 67: 213–246.
- Gould, S.J. 1977. *Ontogeny and Phylogeny*. 501 pp. Harvard University Press, Cambridge.
- Goshe, L.R., Avens, L., Scharf, F.S., and Southwood, A.L. 2010. Estimation of age at maturation and growth of Atlantic green turtles (*Chelonia mydas*) using skeletochronology. *Marine Ecology Progress Series* 157: 1725–1740.
- Guarino, F.M., Andreone, F., and Angelini, F. 1998. Growth and longevity by skeletochronological analysis in *Mantidactylus microtypanum*, a rain-forest anuran from southern Madagascar. *Copeia* 1: 194–198.
- Guillon, J.M., Guery, L., Hulin, V., and Girondot, M. 2012. A large phylogeny of turtles (Testudines) using molecular data. *Contributions to Zoology* 81: 147–158.
- Hansen, J., Sato, M., Russell, G., and Kharecha, P. 2013. Climate sensitivity, sea level and atmospheric carbon dioxide. *Philosophical Transactions of the Royal Society A: Mathematical, Physical and Engineering Sciences* 371: 20120294.
- Hermanson, G., Ferreira, G.S., and Langer, M.C. 2017. The largest Cretaceous podocnemid turtle (Pleurodira) revealed by an isolated plate from the Bauru Basin, south-central Brazil. *Historical Biology* 29: 833–840.
- Hugi, J. and Sánchez-Villagra, M.R. 2012. Life history and skeletal adaptations in the Galapagos marine iguana (*Amblyrhynchus cristatus*) as reconstructed with bone histological data—a comparative study of iguanines. *Journal of Herpetology* 46: 312–324.
- Jannello, J.M., Cerda, I.A., and De la Fuente, M.S. 2016. Shell bone histology of the long-necked chelid *Yaminuechelys* (Testudines: Pleurodira) from the late Cretaceous–early Palaeocene of Patagonia with comments on the histogenesis of bone ornamentation. *The Science of Nature* 103: 26.
- Klein, N. and Sander, P.M. 2007. Bone histology and growth of the prosauropod dinosaur *Plateosaurus engelhardti* von Meyer, 1837 from the Norian bonebeds of Trossingen (Germany) and Frick (Switzerland). *Special Papers in Palaeontology* 77: 169.
- Lescano, J., Bonino, M., and Leynaud, G. 2008. Density, population structure and activity pattern of *Hydromedusa tectifera* (Testudines-Chelidae) in a mountain stream of Córdoba province, Argentina. *Amphibia-Reptilia* 29: 505–512.
- Maniel, I.J. and De la Fuente, M.S. 2016. A review of the fossil record of turtles of the clade Pan-Chelidae. *Bulletin of the Peabody Museum of Natural History* 57: 191–228.
- Maniel, I.J., De la Fuente, M.S., Sterli, J., Jannello, J.M., and Krause, J.M. 2018. New remains of the aquatic turtle *Hydromedusa casamayorensis* (Pleurodira, Chelidae) from the middle Eocene of Patagonia: taxonomic validation and phylogenetic relationships. *Papers in Palaeontology* 4: 537–566.
- Martins, F.I. and Souza, F.L. 2008. Estimates of growth of the Atlantic rain

- forest freshwater turtle *Hydromedusa maximiliani* (Chelidae). *Journal of Herpetology* 42: 54–60.
- Mattox, N.T. 1935. Annular rings in the long bones of turtles and their correlation with size. *Transactions of the Illinois State Academy of Science* 28: 255–256.
- Mikan, J.C. 1820. *Delectus Florae et Faunae Brasiliensis*. 54 pp. Antonii Strauss, Wien.
- Nagy, K.A. 2000. Energy costs of growth in neonate reptiles. *Herpetological Monographs* 14: 378–387.
- Nakajima, Y., Hirayama, R., and Endo, H. 2014. Turtle humeral microanatomy and its relationship to lifestyle. *Biological Journal of the Linnean Society* 112: 719–734.
- Pereyra, M.E., Bona, P., Cerda, I.A., and Desántolo, B. 2019. Osteohistological correlates of muscular attachment in terrestrial and freshwater Testudines. *Journal of Anatomy* 234: 875–898.
- Prieto, A., Martínez-Silvestre, A., Soler, J., Bretones, D., Pascual, E., and Mari, J. 2013. Aportaciones al estudio osteocronológico en un ejemplar de *Testudo hermanni*. *Boletín de la Asociación Herpetológica Española* 57: 934–939.
- Pritchard, P.C.H. 1979. Taxonomy, evolution and zoogeography. In: M. Harless and H. Morlock (eds.), *Turtles: Perspectives and Research*, 1–42. Wiley, New York.
- Pritchard, P.C.H. 1988. A survey of neural bone variation among Recent chelonian species, with functional interpretations. *Acta Zoologica Cracoviensis* 31: 625–686.
- Pritchard, P.C.H. and Trebbau, P. 1984. The turtles of Venezuela. *Society for the Study of Amphibians and Reptiles Contribution to Herpetology* 2: 1–403.
- Rasband, W. 2003. *Image J*. U.S. National Institutes of Health, Bethesda. <http://rsb.info.nih.gov/ij/>
- Reid, R.E.H. 1983. High vascularity in bones of dinosaurs, mammals and birds. *Geological Magazine* 120: 191–194.
- Reid, R.E.H. 1996. Bone histology of the Cleveland-Lloyd dinosaurs and of dinosaurs in general, Part I: Introduction: Introduction to bone tissues. *Brigham Young University Geology Studies* 41: 25–72.
- Reilly, S.M., Wiley, E.O., and Meinhardt, D.J. 1997. An integrative approach to heterochrony: the distinction between interspecific and intraspecific phenomena. *Biological Journal of the Linnean Society* 60: 119–143.
- Rhodin, A.G. 1985. Comparative chondro-osseous development and growth of marine turtles. *Copeia* 1985: 752–771.
- Rootes, W.L., Chabreck, R.H., Wright, V.L., Brown, B.W., and Hess, T.J. 1991. Growth rates of American alligators in estuarine and palustrine wetlands in Louisiana. *Estuaries* 14: 489–494.
- Sander, P.M., Klein, N., Buffetaut, E., Cuny, G., Suteethorn, V., and Le Loeuff, J. 2004. Adaptive radiation in sauropod dinosaurs: bone histology indicates rapid evolution of giant body size through acceleration. *Organisms Diversity and Evolution* 4: 165–173.
- Scheyer, T.M. and Sánchez-Villagra, M.R. 2007. Carapace bone histology in the giant pleurodiran turtle *Stupendemys geographicus*: phylogeny and function. *Acta Palaeontologica Polonica* 52: 137–154.
- Scheyer, T.M., Danilov, I.G., Sukhanov, V.B., and Syromyatnikova, E.V. 2014a. The shell bone histology of fossil and extant marine turtles revisited. *Biological Journal of the Linnean Society* 112: 701–718.
- Scheyer, T.M., Pérez-García, A., and Murelaga, X. 2014b. Shell bone histology of solemydid turtles (stem Testudines): palaeoecological implications. *Organisms Diversity and Evolution* 15: 199–212.
- Schoepff, I.D. 1792. *Historia Testudinum Iconibus Illustrata*. 136 pp. J.J. Palm, Oxford.
- Seddon, J.M., Georges, A., Baverstock, P.R., and McCord, W. 1997. Phylogenetic relationship of chelid turtles (Pleurodira: Chelidae) based on mitochondrial 12S rRNA sequence variation. *Molecular Phylogenetics and Evolution* 7: 55–61.
- Shine, R. and Iverson, J.B. 1995. Patterns of survival, growth, and maturation in turtles. *Oikos* 72: 343–348.
- Schneider, J.G. 1783. *Allgemeine Naturgeschichte der Schildkröten, nebst einem systematischen Verzeichnisse der einzelnen Arten*. 364 pp. J.G. Müller, Leipzig.
- Schweigger, A.E. 1812. Prodrum monographie Cheloniorum. *Königsberger Archiv für Naturwissenschaft und Mathematik* 1812: 271–458.
- Staesche, K. 1929. Schildkrötenreste aus der oberen Kreide Patagoniens. *Palaeontographica A* 72: 103–112.
- Sterli, J. and De la Fuente, M.S. 2013. New evidence from the Palaeocene of Patagonia (Argentina) on the evolution and palaeo-biogeography of Meiolaniformes (Testudinata, new taxon name). *Journal of Systematic Palaeontology* 11: 835–852.
- Suzuki, H.K. 1963. Studies on the osseous system of the slider turtle. *Annals New York Academy of Sciences* 109: 351–410.
- Tutiempo Network, S.L. 2019. *Climate Information for All Countries of the World With Historical Data*. <https://www.tutiempo.net/clima/ws-875930.html> (accessed 3 October 2019).
- Vlachos, E. and Rabi, M. 2018. Total evidence analysis and body size evolution of extant and extinct tortoises (Testudines: Cryptodira: Pan-Testudinidae). *Cladistics* 34: 652–683.
- Wagler, J. 1830. *Natürliches System der Amphibien, mit vorangehender Classification der Säugthiere und Vogel. Ein Beitrag zur vergleichenden Zoologie*. 354 pp. J.G. Cotta'schen Buchhandlung, Munich.
- Wells, J.W. 1963. Coral growth and geochronometry. *Nature* 197: 948–950.
- Woodward, H.N., Horner, J.R., and Farlow, J.O. 2014. Quantification of intraskeletal histovariability in *Alligator mississippiensis* and implications for vertebrate osteohistology. *PeerJ* 2: e422.
- Zachos, J.C., Dickens, G.R., and Zeebe, R.E. 2008. An Early Cenozoic perspective on greenhouse warming and carbon-cycle dynamics. *Nature* 451: 279–283.
- Zug, G.R., Balazs, G.H., and Wetherall, J.A. 1995. Growth in juvenile loggerhead seaturtles (*Caretta caretta*) in the north Pacific pelagic habitat. *Copeia* 1995: 484–487.
- Zug, G.R., Chaloupka, M., and Balazs, G.H. 2006. Age and growth in olive ridley seaturtles (*Lepidochelys olivacea*) from the North-central Pacific: a skeletochronological analysis. *Marine Ecology* 27: 263–270.